Photoaffinity Labeling of *Torpedo* Nicotinic Receptor with the Agonist [^{3}H]DCTA: Identification of Amino Acid Residues Which Contribute to the Binding of the Ester Moiety of Acetylcholine†

Thomas Grutter,‡ Laurence Ehret-Sabatier,§ Florence Kotzyba-Hibert,*,‡ and Maurice Goeldner‡

Laboratoire de Chimie Bio-Organique, UMR 7514 CNRS, Faculté de Pharmacie, Université Louis Pasteur, Strasbourg, 74 route du Rhin, BP 24, 67401 Illkirch Cedex, France, and Laboratoire de Réponse Immunitaire et Développement chez les Insectes, UPR 9022 CNRS, Institut de Biologie Moléculaire et Cellulaire, Université Louis Pasteur, Strasbourg, 15 rue Descartes, 67084 Strasbourg Cedex, France

Received October 14, 1999; Revised Manuscript Received December 8, 1999

ABSTRACT: *Torpedo marmorata* acetylcholine binding sites were photolabeled using 360 nm light, at equilibrium in the desensitized state, with the agonist [^{3}H]DCTA utilizing the Ce^{IV}/glutathione procedure described previously (Grutter, et al. (1999) *Biochemistry 38,* 7476−7484). Photoincorporation of [^{3}H]-DCTA was concentration-dependent with a maximum of 7.5% specific labeling on the α-subunit and 1.2% on the γ-subunit. The apparent dissociation constants for labeling of the α- and γ-subunits were 2.2 ± 1.1 and 3.6 ± 2.8 μM, respectively. The α-chains isolated from receptor-rich membranes photolabeled in the absence or in the presence of carbamylcholine were cleaved with CNBr using an efficient "in gel" procedure. The resulting peptide fragments were purified by HPLC and further submitted to trypsinolysis. The digest was analyzed by HPLC leading to a single radioactive peak which, by microsequencing, revealed two sequences extending from αLys-179 and from αHis-186, respectively. Radioactive signals could be unambiguously attributed to positions corresponding to residues αTyr-190, αCys-192, αCys-193, and αTyr-198. These four identified [^{3}H]DCTA-labeled residues, which have been also labeled with other affinity and photoaffinity probes including the agonist [^{3}H]nicotine, belong to loop C of the ACh binding site. The chemical structure of [^{3}H]DCTA, together with its well-defined and powerful photochemical reactivity, provides convincing evidence that loop C-labeled residues are primarily involved in the interaction with the ester moiety of acetylcholine.

The nicotinic acetylcholine receptor (nAChR)[1] from fish electric organ and vertebrate neuromuscular junction is a well-characterized transmembrane allosteric protein (*1*) composed of four polypeptide chains assembled into a heterologous $(\alpha1)_2(\beta1)\gamma\delta$ pentamer (*2*) which carries the acetylcholine (ACh) binding sites and contains the cation-selective channel-forming elements (*3*, *4*). The molecular structure of the *Torpedo marmorata* ACh binding site has been probed by site-directed irreversible photolabeling experiments using photosensitive antagonists [^{3}H]DDF (*5*, *6*) and [^{3}H]*d*-tubocurarine (*7*) or agonist [^{3}H]nicotine (*8*). In addition, site-directed affinity probes including [^{3}H]-lophotoxin analog-1 (*9*), [^{3}H]MBTA (*10*), and [^{3}H]ACh mustard (*11*) targeted nucleophilic residue(s) within the binding site. From these different topographical mapping studies three domains of the α-subunit centered around loop A (αTyr-93), loop B (αTrp-149), and loop C (αTyr-190, αCys-192, αCys-193, αTyr-198) have been defined. Residues γTrp-55, γTyr-111, γTyr-117, and δTrp-57 were also identified as the sites of specific [^{3}H]*d*-tubocurarine photoincorporation (*7*, *12*) while residue γTrp-55 was identified by the agonist [^{3}H]nicotine (*13*), demonstrating that other subunits (γ and/or δ) are associated with the α-subunit to form a functional agonist binding site.

However, the precise positioning of the ACh molecule within these binding domains remains to be defined and constitutes a further objective. While the DDF molecule possessed remarkable photochemical properties, this probe, due to its chemical structure, targeted very broadly the ammonium binding site. Alternatively, the other photoaffinity probes, including *d*-tubocurarine and nicotine, were lacking defined photochemical properties preventing therefore the

† This work was supported by the Centre National de la Recherche Scientifique, the Région Alsace, the Association Française contre les Myopathies, Naturalia et Biologia.

* To whom correspondence should be addressed. E-mail: kotzyba@bioorga.u-strasbg.fr.

‡ Laboratoire de Chimie Bio-Organique, Université Louis Pasteur, Strasbourg. Phone: 333 88676838. Fax: 333 88678891. E-mail: grutter@bioorga.u-strasbg.fr; goeldner@bioorga.u-strasbg.fr.

§ Laboratoire de Réponse Immunitaire et Développement chez les Insectes, Université Louis Pasteur, Strasbourg. E-mail: sabatier@ibmc.u-strasbg.fr.

[1] Abbreviations: nAChR, nicotinic acetylcholine receptor; ACh, acetylcholine; CCh, carbamylcholine; DDF, *p*-(*N*,*N*-dimethylamino)-benzenediazonium fluoroborate; DCTA, (diazocyclohexadienoylpropyl)-trimethylammonium; α-BgTx, α-bungarotoxin; GSH, reduced glutathione; Ce^{IV}, cerium nitrate ammonium $(Ce^{IV}(NH_4)_2(NO_3)_6)$; DTT, dithiothreitol; SDS, sodium dodecyl sulfate; TFA, trifluoroacetic acid; HPLC, high-performance liquid chromatography; PAGE, polyacrylamide gel electrophoresis; PNGase F, peptide *N*-glycosidase F; CBB, coomassie brillant blue; CNBr, cyanogen bromide; ACN, acetonitrile; PB, sodium phosphate buffer; PTH amino acids, phenyl thiohydantoin amino acids.

10.1021/bi992393o CCC: $19.00
Published on Web 02/25/2000

Chart 1: Chemical Structure of the Agonists ACh and [^{3}H]DCTA[a]

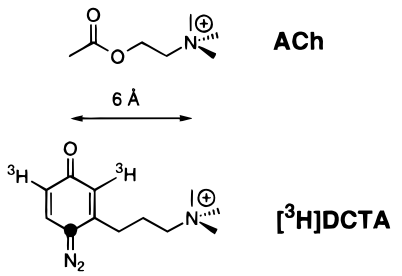

[a] The filled circle identifies the reactive carbon of the photoactivated species (carbene) of DCTA. A maximum of 6 Å separates this carbon from the quaternary nitrogen.

generation of a molecular link between the labeled amino acids and the probe. For this purpose, we recently developed a novel family of photosensitive agonists, of suitable size and reactivity, designed to incorporate instantaneously and covalently, upon UV irradiation, in surrounding residues (*14*). One of these photoprobes DCTA (Chart 1), which was shown to be a functional agonist (*15*), carried, in addition to the quaternary ammonium group desirable for cholinergic recognition, a highly photosensitive 4-diazocyclohexa-2,5-dienone moiety designed to probe the ACh ester-binding pocket. [^{3}H]DCTA was synthesized and used to photoalkylate the ACh binding sites of *Torpedo* nAChR (*15*, *16*).

In this paper, we analyzed, at the molecular level, the photoaffinity labeling experiments done on desensitized *Torpedo* nAChR using the agonist [^{3}H]DCTA. Proteolysis of the α-subunit with CNBr, using an efficient "in gel" procedure, was followed by trypsinolysis. The radiolabeled peptides were purified and analyzed by microsequencing, allowing unambiguous identification of residues αTyr-190, αCys-192, αCys-193, and αTyr-198 as being specifically alkylated by [^{3}H]DCTA. On the basis of our labeling results, we propose that loop C is part of the ester subsite of the ACh binding site.

MATERIALS AND METHODS

Materials. [^{3}H]DCTA (0.65 Ci/mmol) was synthesized and purified as described previously (*15*). [^{125}I]α-bungarotoxin ([^{125}I]α-BgTx) was purchased from New England Nuclear. Small live *Torpedo marmorata* fishes were obtained from the Biological Station of Roscoff, France. Electric organs were dissected, liquid nitrogen frozen, and stored at −80 °C. Pepstatin, aprotinin, PMSF, proadifen, carbamylcholine (CCh), *d*-tubocurarine chloride, reduced glutathione (GSH), dithiothreitol (DTT), coomassie brillant blue (CBB), and *n*-octyl-*β*-D-glucopyranoside were purchased from Sigma. Cerium nitrate ammonium ($Ce^{IV}(NH_4)_2(NO_3)_6$) was purchased from Janssen. CNBr was purchased from Aldrich, and porcine pancreatic trypsin (sequencing grade modified) was from Promega. Recombinant *N*-glycosidase F (PNGase F) was obtained in our laboratory as described previously (*17*).

Membrane Preparation. nAChR-rich membrane fragments were purified from *T. marmorata* frozen electric organs as described elsewhere (*18*) except for the buffer which was 50 mM PB pH 7.5. Further purification was achieved by alkali treatment of nAChR-rich membrane (*19*). Specific [^{125}I]α-BgTx binding was determined by the DEAE filter disk procedure and typically ranged from 3 to 4 nmol of [^{125}I]α-BgTx bound per mg of protein (*20*). Protein determination was achieved by a modified Lowry method (*21*).

Photolabeling of nAChR-Rich Membranes with [^{3}H]DCTA. Photololabeling of nAChR-rich membranes with [^{3}H]DCTA was achieved as described previously (*16*). For analytical photolabeling experiments, alkaline-treated membranes (60 μg, 210 pmol of α-BgTx binding sites) were suspended in 10 mM PB pH 7.2 (600 μL), preincubated with 15 μM proadifen (50 min at room temperature), and mixed with various concentrations of [^{3}H]DCTA (from 2.5 to 50 μM) in the presence of 500 μM Ce^{IV}/100 μM GSH as photolysis byproduct scavengers. The samples were irradiated at 360 nm (30 μV) for 20 min at room temperature. Protection experiments were carried out with prior addition of either *d*-tubocurarine (various concentrations from 0.01 to 100 μM, 30 min at room temperature) or CCh (100 μM, 30 min at room temperature). Preparative photolabeling of large amounts (∼320−600 μg of α-subunits, 8−15 nmol of α-Bgtx binding sites) of alkaline-treated nAChR-rich membranes were achieved at 360 nm (75 μV) for 20 min and required 20 successive labeling experiments. Final concentrations during each irradiation (1.5 mL) were 0.5 μM α-Bgtx binding sites with 10 μM [^{3}H]DCTA/500 μM Ce^{IV}/100 μM GSH added after 50 min preincubation with 15 μM proadifen and when indicated 100 μM CCh (30 min pretreatment before irradiation).

Following irradiation, photolabeled nAChRs were recovered after one-step centrifugation (11 000*g*, 30 min, 4 °C) and pellets were solubilized in the Laemmli sample buffer. For analytical photolabeling, the solubilized membranes were analyzed on 10% SDS−PAGE and radioactivity into each polypeptide chain was quantified as described (*16*, *22*). For preparative photolabeling, aliquots of the solubilized membranes were analyzed on 10% SDS−PAGE and the radioactivity incorporated was quantified as mentioned above.

Isolation of [^{3}H]DCTA-Labeled α-Subunit. Solubilized membranes were subjected to preparative 10% SDS−PAGE. The gel was stained for 20 min with an aqueous solution containing 0.05% CBB (R-250), 25% methanol, and 5% acetic acid and then destained with 30% methanol aqueous solution according to a modified procedure from Rosenfeld et al. (*23*). The corresponding α-subunit (2−3 nmol) was excised, cut into pieces, transferred to an Eppendorf tube, and washed twice under vigorous shaking, with 450 μL of 50% ACN aqueous solution at room temperature for 10 min. The supernatants were put aside, and the gel pieces were dried under vacuum in a Speed-Vac centrifuge (Savant) at room temperature and rehydrated with 450 μL of water followed by immediate addition of 5 μL of a 10 mM DTT aqueous solution. After 30 min at 30 °C, the α-subunit was treated, for 30 min at room temperature in the absence of light, with 5 μL of a 25 mM iodoacetamide aqueous solution. After a repeated wash under vigorous shaking using a 50% ACN aqueous solution and removing supernatants, the gel pieces were dried under vacuum in a Speed-Vac centrifuge. During all these steps, less than 5% radioactivity was released in the supernatants. We also checked that the α-subunit was not eluted from the gel pieces under these conditions.

"In Gel" CNBr Cleavage of the α-Subunit and Peptides Purification. The dried gel pieces were rehydrated within 5 min by three successive additions of 50 μL of CNBr solution

(16 μg/μL in 70% formic acid), followed by an addition of 70% formic acid sufficient to soak the gel pieces (700 μL), and the samples were kept in the dark at room temperature under argon for 60 h (*24*, *25*). The samples were washed twice with 500 μL of water, evaporated each time in a Speed-Vac centrifuge. The CNBr digests were extracted from the gel pieces by successive treatment with solutions containing 2 × 250 μL of 0.1% TFA in H_2O/50% ACN under vigorous shaking for 80 min each and 2 × 250 μL of 0.1% TFA in H_2O/15% ACN/35% 1-propanol/0.1% *n*-octyl-β-D-glucopyranoside under vigorous shaking for 2 days. The recovery of the radioactivity found in pooled supernatants, following extraction, ranged from 55 to 65%.

The supernatants were concentrated to a final volume of approximately 80 μL using a gentle nitrogen (N_2) flux, before adding 350 μL of an aqueous solution containing 0.1% TFA/7% 1-propanol/3% ACN. The crude reaction mixture was loaded onto a reversed-phase HPLC column: Vydac C4, 2.1 × 150 mm (0.2 mL/min) or 4.6 × 250 mm (1 mL/min; see figure legends) equilibrated with 95% solvent A (0.1% TFA in H_2O) and 5% solvent B (70% 1-propanol, 30% ACN, 0.095% TFA). After injection, development at 5% solvent B for 15 min was followed by a linear gradient from 5 to 60% solvent B over 160 min, followed by a linear gradient from 60% to 100% solvent B over 30 min. UV absorbance was monitored at 214 nm, and aliquots of collected fractions were counted for radioactivity.

Trypsin Subcleavage of CNBr Fragments. Purified [^{3}H]-DCTA-labeled CNBr fragments were neutralized with 2 N NaOH at 4 °C, evaporated under N_2, and diluted (approximately 0.5 mg/mL) in 150 mM NH_4HCO_3 pH 7.8 and 30% ACN. Trypsin was added (1/50 w/w), and the mixture was incubated for 14 h at 28 °C. After acidification with solvent A (0.1% TFA in H_2O), the mixture was loaded onto the Vydac C4 column (2.1 × 150 mm) and eluted as indicated previously.

Peptide Sequencing. The HPLC-purified fractions were pooled, evaporated under N_2 until 10−15 μL, and loaded to the biobrene pretreated filter of the sequenator. A 20 μL volume of 50% ACN/50% formic acid was further added to the tube, vigorously shaked, and loaded. Automated Edman degradation was performed on a pulse liquid automated sequenator (Applied Biosystems model 473A). The remaining HPLC output from each cycle was collected and counted for radioactivity quantification.

Deglycosylation of CNBr Fragments. Aliquots of [^{3}H]-DCTA-labeled CNBr fragments were evaporated under N_2 and neutralized (approximately 0.05 mg/mL) with 50 mM NH_4HCO_3 pH 7.8 and 0.25% *n*-octyl-β-D-glucopyranoside. PNGase F was added (1/40 w/w), and the mixture was incubated for 6 h at room temperature. The crude reaction was analyzed either by 19% Tricine SDS−PAGE (*26*) or by HPLC using the narrow bore column and elution system as described previously. For 19% Tricine SDS−PAGE, the incorporated radioactivity was quantified after gel slicing, digestion, and counting (*22*).

Data Analysis. Concentration dependence of subunits photolabeling was fitted by the nonlinear least-squares program (Sigma Plot, Jandel) according to a single-site binding function [$B = A/(1 + (K_{irr}/L))$], where B is the specific photoincorporation of [^{3}H]DCTA, A is the maximum specific photoincorporation, K_{app} is the apparent dissociation constant, and L is the [^{3}H]DCTA concentration. Inhibition of [^{3}H]DCTA photolabeling by *d*-tubocurarine was fitted to the experimental data according to either a single-site [$B = A/(1 + (I/K)^{n_H}) + NS$] or a two-sites [$B = \alpha(A/(1 + (I/K_1)^{n_{H1}})) + (1 - \alpha)(A/(1 + (I/K_2)^{n_{H2}})) + NS$] model, where B is the photoincorporation of [^{3}H]DCTA, α is the fraction of high-affinity sites and $1 - \alpha$ is the fraction of low-affinity sites, A is the maximum photoincorporation of [^{3}H]DCTA (e. g. in the absence of *d*-tubocurarine) for the [^{3}H]DCTA concentration used, K is the concentration of *d*-tubocurarine that yields 50% inhibition, n_H is the Hill coefficient, I is the *d*-tubocurarine concentration, and NS is the nonspecific photolabeling.

For sequence analysis, initial peptide mass (I_0) and repetitive yields (R) were calculated by linear least-squares analysis of the function $\log I_n = n[\log R] + \log I_0$, where I_n is the observed PTH amino acid mass released in cycle n.

RESULTS

Photoincorporation of [^{3}H]DCTA into nAChR-Rich Membranes. In a previous study, it was shown that, during the photolabeling experiments of nAChR-rich membranes using [^{3}H]DCTA, side reactions occurred which generated nonspecific labeling. We overcame these major drawbacks by quenching rapidly these nondesired reactions using subsequent addition of the oxidant ceric ion (Ce^{IV}) and reduced glutathione (GSH), leading to a very efficient and specific photolabeling reaction (*16*). We tested these new experimental conditions at different probe concentrations ranging from 2.5 to 50 μM. The concentration dependence of [^{3}H]-DCTA photoincorporation into both the α- and γ-subunits was measured at equilibrium, in the presence of proadifen (15 μM), conditions where the receptor is mainly in the high-affinity D state [75% D, 25% R (*27*, *28*)]. Figure 1A shows that nonspecific labeling (e.g. in the presence of 100 μM CCh) was a linear function of [^{3}H]DCTA concentration at least up to 50 μM. The K_{app}'s for specific photolabeling of the α- and γ-subunits were 2.2 ± 1.1 and 3.6 ± 2.8 μM, respectively. The maximum specific photoincorporation values were 116 ± 14 and 19.0 ± 3.4 dpm/pmol for α- and γ-subunits, respectively (Figure 1A). These values represent 7.5% of specific labeling of the binding sites for the α-subunit and 1.2% for the γ-subunit (specific radioactivity of [^{3}H]DCTA: 1430 dpm/pmol).

The inhibition of photolabeling by *d*-tubocurarine was studied to determine the relative contribution of the γ-subunit compared to the α-subunit in the high- and low-affinity site of *d*-tubocurarine. The inhibition of [^{3}H]DCTA photoincorporation by *d*-tubocurarine was slightly different for the α- and γ-subunits (Figure 1B). For the α-subunit, a single-site model gave a dissociation constant $K = 0.50$ μM with a Hill coefficient $n_H = 0.75$. Using a two-sites model, the best fit gave 59% (see Materials and Methods) of high-affinity site with $K_1 = 0.38$ μM, $n_{H1} = 1.30$ and 41% of low-affinity site with $K_2 = 14$ μM, $n_{H2} = 0.15$. For the γ-subunit, the best fit is obtained with a single-site model with $K = 0.20$ μM and $n_H = 1.15$. These values are close to those determined for [^{3}H]nicotine (*8*) and consistent with the hypothesis that the γ-subunit contributes to the high-affinity *d*-tubocurarine site, whereas the δ-subunit (which was not alkylated by [^{3}H]DCTA (*16*)) would be part of its low-affinity site (*29*, *30*).

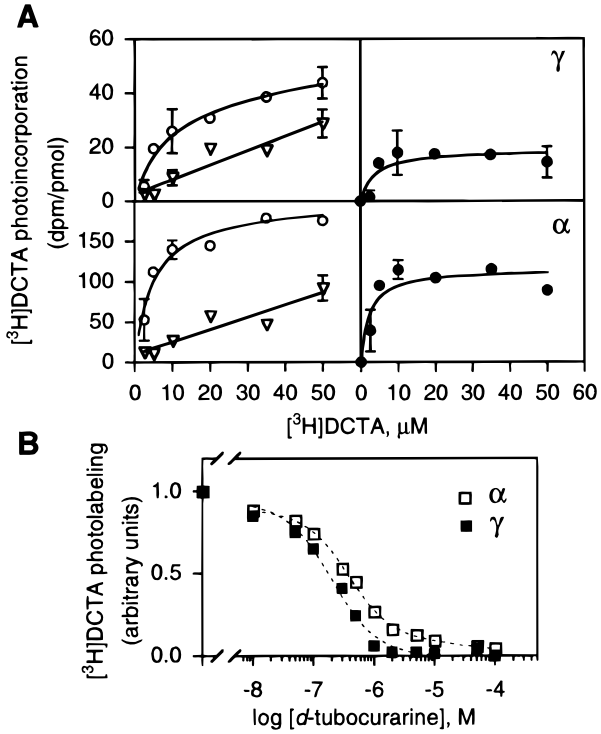

FIGURE 1: Analysis of [^{3}H]DCTA photoincorporation into nAChR-rich membranes. (A) Concentration dependence of [^{3}H]DCTA photolabeling into the α- and γ-subunits. Alkaline-treated membranes (210 pmol, 0.35 μM of α-BgTx binding sites) were preincubated with 15 μM proadifen for 50 min at room temperature, mixed with various concentrations of [^{3}H]DCTA (from 2.5 to 50 μM) supplemented with 500 μM Ce^{IV}/100 μM GSH, and irradiated at 360 nm for 20 min in the presence (▽) or absence (○) of 100 μM CCh. After irradiation, the samples were centrifuged (11 000*g*, for 30 min, 4 °C), and pellets were subjected to 10% SDS−PAGE. Distribution of the radioactivity into the α- and γ-subunits was measured after gel slicing, digestion, and counting. The specific photolabeling which is the difference between the total (○) and the calculated nonspecific photolabeling (obtained from linear least-squares analysis of experimental data (▽)) is given by ●. Symbols represent the average (±SD) of duplicate (in some case triplicate) determinations, and for the specific photolabeling, the solid lines are fitted to the data by nonlinear least-squares analysis according to a single-site model (see Materials and Methods). The K_{app}'s for specific photolabeling of the α- and γ-subunits were 2.2 ± 1.1 and 3.6 ± 2.8 μM, respectively. The maximum specific photoincorporation were 116 ± 14 and 19.0 ± 3.4 dpm/pmol for α- and γ-subunits, respectively. (B) Inhibition of [^{3}H]DCTA photoincorporation into the α- and γ-subunits by *d*-tubocurarine. Alkaline-treated membranes (210 pmol, 0.35 μM of α-BgTx binding sites) were preincubated with 15 μM proadifen for 50 min and irradiated with 10 μM [^{3}H]DCTA/500 μM Ce^{IV}/100 μM GSH as mentioned above in the absence or presence of various concentrations of *d*-tubocurarine. Distribution of the radioactivity into the α- (□) and γ- (■) subunits was determined as described above. Data were normalized to the labeling in the absence of *d*-tubocurarine, and the dashed lines were fitted to the data by nonlinear least-squares analysis according to a single-site or a two-sites model for γ- and α-subunits, respectively (see Materials and Methods). For the α-subunit, a single-site model gave a dissociation constant $K = 0.50$ μM with a Hill coefficient $n_H = 0.75$. Using a two-sites model, the best fit gave 59% of high-affinity site with $K_1 = 0.38$ μM, $n_{H1} = 1.30$ and 41% of low-affinity site with $K_2 = 14$ μM, $n_{H2} = 0.15$. For the γ-subunit, the best fit is obtained with a single-site model with $K = 0.20$ μM and $n_H = 1.15$.

Identification of [^{3}H]DCTA-Labeled α-Subunit Residues. Preparative photolabeling at equilibrium of *Torpedo* alkaline-treated membranes preincubated with proadifen was achieved as described under Materials and Methods. In these preparative photolabeling conditions, yields of photocoupling and protection by 100 μM CCh were similar to those observed in analytical experiments (not shown). To localize the sites of photoincorporation, [^{3}H]DCTA-labeled α-subunit was digested directly "in gel" with CNBr, according to a modified procedure of Cordoba et al. (*25*). The "in gel" method was first described for trypsinolysis (*23*) and extended to CNBr proteolysis (*24*, *25*), and this procedure was applied here, for the first time, to the *Torpedo* nicotinic acetylcholine receptor. This method represents a convenient procedure leading to satisfactory yields since the recovery of radioactivity after digestion and fragments extraction ranged between 55 and 65%. The material which could not be eluted from the gel pieces probably corresponded to aggregated protein due to the presence of formic acid.

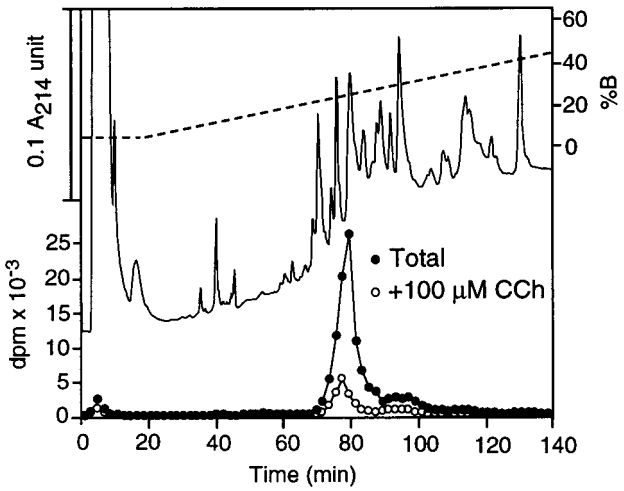

FIGURE 2: Reversed-phase HPLC of CNBr digests of the [^{3}H]-DCTA-labeled α-subunit. Large amounts of alkaline-treated membranes (8 nmol, 0.5 μM of α-BgTx binding sites) were preincubated with 15 μM proadifen for 50 min at room temperature, mixed with 10 μM [^{3}H]DCTA/500 μM Ce^{IV}/100 μM GSH, and irradiated at 360 nm for 20 min in the presence (○) or absence (●) of 100 μM CCh. After irradiation, the samples were centrifuged (11 000*g*, for 30 min, 4 °C), and pellets were subjected to preparative 10% SDS−PAGE. The [^{3}H]DCTA-labeled α-subunit was excised, reduced, alkylated, and cleaved "in gel" with CNBr (see Materials and Methods). The CNBr digests were extracted and injected (~40 μg of α-subunit for each injection) onto a Vydac C4 reversed-phase column (2.1 × 250 mm) equilibrated with 95% solvent A (0.1% TFA in H_2O) and 5% solvent B (70% 1-propanol, 30% ACN, 0.095% TFA). After injection, the column was eluted at 0.2 mL/min with 5% solvent B for 15 min, followed by a linear gradient from 5 to 60% solvent B over 160 min. UV absorbance was monitored at 214 nm, and aliquots of collected fractions were counted for radioactivity. The recovery of injected radioactivity was 90−95% for each of the sample irradiated in the absence of CCh. Radiolabeled peptides contained in fractions 77−81 min were evaporated under N_2 and subjected to sequence analysis.

When the eluates were loaded on reversed-phase HPLC, less than 4% of the injected radioactivity was released in the void volume (this material was not further analyzed) while a single radioactive peak eluting around 26−27% of solvent B was associated with a large UV_{214} absorption peak (Figure 2). This radioactive peak was reduced by 75% in the presence of 100 μM CCh, and no other significant radioactive peak was observed up to 100% solvent B, leading to 90−95% overall radioactivity recovery. Fractions eluting between 77 and 81 min were pooled and analyzed for sequencing.

Table 1: Yields of PTH Amino Acids upon Sequence Analysis of CNBr Peptides

	PTH amino acids (pmol)				
cycle	I	II	III	IV	V
1	K (NQ)[a]	E (NQ)	V (NQ)	W (NQ)	K (NQ)
2	D (NQ)	S (ND)[b]	I (34)	T (38)	L (4.4)
3	Y (62)	G (12)[c]	D (NQ)	P (51)	G (12)[c]
4	R (29)	E (9.7)	H (19)	P (13)	I (3.9)
5	G (36)	W (ND)	I (25)	A (155)	W (ND)
6	W (0.8)	V (6.5)	L (30)	I (46)	T (1.7)
7	K (19)	M (4.9)	L (8.0)	F (76)	Y (8.4)
8	H (12)	K (43)[c]	C (ND)	K (43)[c]	D (2.3)
9	W (2.4)	D (3.3)	V (18)	S (32)	G (12)
10	V (17)	Y (111)[c]	F (ND)	Y (111)[c]	T (3.3)
11	Y (NQ)	R (2.6)		C (ND)	K (ND)
12	Y (NQ)	G (12)		E (32)	V (2.0)
13	T (6.9)	W (ND)		I (57)	S (1.4)
14	C (ND)	K (0.9)		I (26)[c]	I (26)[c]
15	C (ND)	H (1.1)		V (97)	S (1.7)
16	P (5.1)[c]	W (ND)		T (34)	P (5.1)[c]
17	D (2.4)	V (ND)		H (29)	E (ND)
18	T (ND)	Y (3.7)		F (55)	S (1.8)
19	P (25)[c]	Y (ND)		P (25)[c]	D (ND)
20	Y (3.1)	T (ND)		F (20)	R (1.3)
21	L (3.9)	C (ND)		D (21)	P (ND)
22	D (1.5)[c]	C (ND)		Q (31)	D (1.5)[c]
23	I (2.4)	P (ND)		Q (20)	L (ND)
24	T (2.3)	D (ND)		N (ND)	S (1.4)
25	Y (1.5)	T (0.1)[c]		C (ND)	T (0.1)[c]
26	H (0.5)	P (ND)		T (5.1)	F (ND)
initial amt (I_0, pmol)	66	12	38	68	6.9
repetitive yield (R, %)	85	90	89	95	92
starting posn	α179	α172	α405	α118	α145

[a] NQ indicates that the residue was detected but not quantified because of first cycle or of carry over from the same residue present in preeceding cycle. [b] ND indicates that the residue was not identified but deduced from sequence. [c] Residues that were present in different sequences were not included in the linear regression analysis for the calculation of the repetitive yield and initial amount.

Sequence analysis of the single radioactive peak revealed five amino-terminal sequences corresponding to α-subunit CNBr fragments (Table 1). This mixture was composed of two predominant sequences extending from αLys-179 (66 pmol) and αTrp-118 (68 pmol), two minor sequences extending from αLys-145 (6.9 pmol) and αGlu-172 (12 pmol), and a last sequence extending from αVal-405 which stopped after 11 cycles. The radioactivity measurements on the sequenator output revealed release of tritium at cycles 12, 14, 15, 20, 21, and 22, respectively (Figure 3).

To determine which peptide(s) and amino acid(s) carried the radioactivity, we took advantage of the fact that there was a single site of N-linked carbohydrate in the α-subunit (αAsn-141) belonging to the identified peptide αTrp-118 (the next Met residue being at position 144). When the CNBr fragments were treated with PNGase F and subjected to reversed-phase HPLC using the same elution system as described (Figure 4A), no significant shift in the retention time of the radioactive peak was detected when compared to the untreated sample (Figure 2), whereas the large UV_{214} absorption peak decreased strongly (see arrow in Figure 4A) suggesting that this peak could correspond to the peptide αTrp-118 containing the glycosylation site. Furthermore, these PNGase F treated CNBr fragments, along with an untreated control, were also analyzed by 19% Tricine SDS−PAGE, and the distribution of radioactivity was determined by gel slice analysis (*22*). In the PNGase F treated CNBr fragments, a single peak of about 6 kDa was observed which

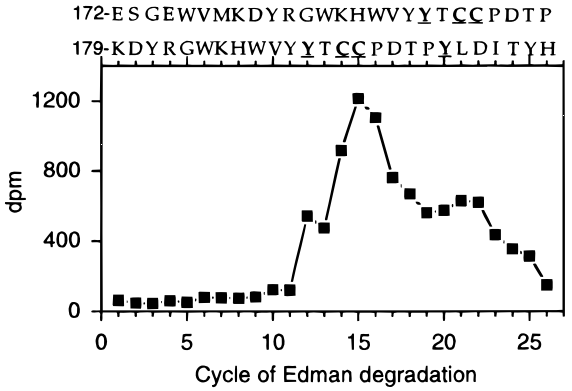

FIGURE 3: Radioactivity released upon sequential Edman degradation of [^{3}H]DCTA-labeled CNBr fragments. Purified material eluting between 77 and 81 min (Figure 2) was subjected to automated sequence analysis. Radioactivity associated with the PTH fraction at each cycle is shown (■). The loaded sample contained approximately 8.5×10^4 dpm, of which 8.5% remained on the filter after 26 cycles. The total radioactivity recovered in the 26 cycles represented 12.3×10^2 dpm (15% of the load). The two identified peptides extending from αLys-179 and αGlu-172 are shown, and the radiolabeled amino acids are indicated in underlined and boldface type.

did not differ significantly (the expected apparent shift is at least 2 kDa) from the untreated sample (Figure 4B). Altogether, these results suggest that the peptide extending from αTrp-118 does not contain the radioactivity.

The release of radioactivity did not originate from the CNBr fragment begining at αLys-145 since the ratio of specific release of tritium to the mass of PTH amino acids detected for this sequence (2100 dpm/pmol) would exceed the specific radioactivity of [^{3}H]DCTA (0.65 Ci/mmol that is 1430 dpm/pmol).

Although the pattern of tritium release was complex, it appeared that the radioactivity measured corresponded to either αLys-179 or αGlu-172 peptides or both. These two peptides contain an overlapping sequence starting at αLys-179; therefore, the labeled PTH amino acid in cycle 12 cannot correspond to residue αGly-183 since no radioactivity release was detected in cycle 5, as would have been otherwise observed (Figure 3). Consequently, the tritium was released from residue αTyr-190 in the peptide extending from αLys-179. For similar reasons, radioactivity released at cycles 14 and 15 can be attributed to residues αCys-192 and αCys-193 belonging to the same αLys-179 extending peptide. Also, the observed radioactivity release at cycles 21 and 22 (Figure 3) is best explained by labeling of the same two Cys residues within peptide αGlu-172. Finally, the weak radioactivity increase at cycle 20 can be tentatively attributed to the labeling of αTyr-198. These results not only needed to be confirmed but also, even if unlikely, it remained possible that part of the observed tritium release did originate from some contaminating peptide, not detectable by sequence analysis.

To confirm whether αTyr-190, αCys-192, αCys-193, and eventually αTyr-198 represented sites of [^{3}H]DCTA specific photoincorporation, the unique CNBr peak was further subcleaved with trypsin and the fragments were purified by reversed-phase HPLC. Approximately 20% of the radioactivity recovered from the HPLC column eluted with unbound material (Figure 5). The labeling of this material was decreased by 57% in the carbamylcholine-protected

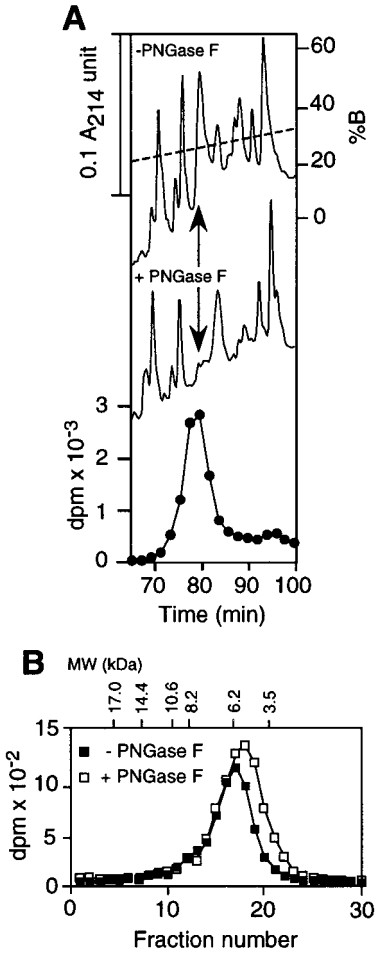

FIGURE 4: Deglycosylation of the CNBr fragment extending from αTrp-118. Alkaline-treated membranes were photolabeled with [^{3}H]-DCTA as described in Figure 2. The [^{3}H]DCTA-labeled α-subunit was cleaved "in gel" with CNBr as mentioned in Materials and Methods. Aliquots of the CNBr-extracted digests were either treated with PNGase F (1/40 w/w) for 6 h at room temperature or not treated (control). The crude reaction was analyzed either (A) by HLPC or (B) by 19% Tricine SDS−PAGE. (A) The reaction medium was injected onto a Vydac C4 reversed-phase column (2.1 × 250 mm) equilibrated with 95% solvent A (0.1% TFA in H_2O) and 5% solvent B (70% 1-propanol, 30% ACN, 0.095% TFA). The elution was performed as described in Figure 2. Top: UV absorbance profile at 214 nm for the untreated sample. Middle: UV absorbance profile at 214 nm for the PNGase F treated sample. Bottom: Distribution of the radioactivity for the PNGase F treated CNBr fragments. For radioactivity comparison, see Figure 2. (B) The deglycosylated sample (□) and the control sample (■) were loaded on 19% Tricine SDS−PAGE. The distribution of radioactivity was measured by gel slicing, digestion, and counting. Also indicated are the molecular weight markers (MW in kDa). The standards used were myoglobin (1−153, 17 kDa), myoglobin I + II (1−131, 14.4 kDa), myoglobin I + III (56−153, 10.6 kDa), myoglobin I (56−131, 8.2 kDa), myoglobin II (1−55, 6.2 kDa), and glucagon (3.5 kDa).

sample. This material was not further characterized. A second peak of radioactivity (93% protection by carbamylcholine) was eluted from the column around 26−27% of solvent B. The purified material eluting between 76 and 79 min was pooled and subjected to Edman degradation. The major peptide sequence extending from αVal-405 was still present (absence of specific cleavage site for trypsin) but did not interfere with the identification of the labeled amino acids. Three overlapping amino-terminal sequences extending from αHis-186, αLys-179, and αGlu-172, were present (Table 2).

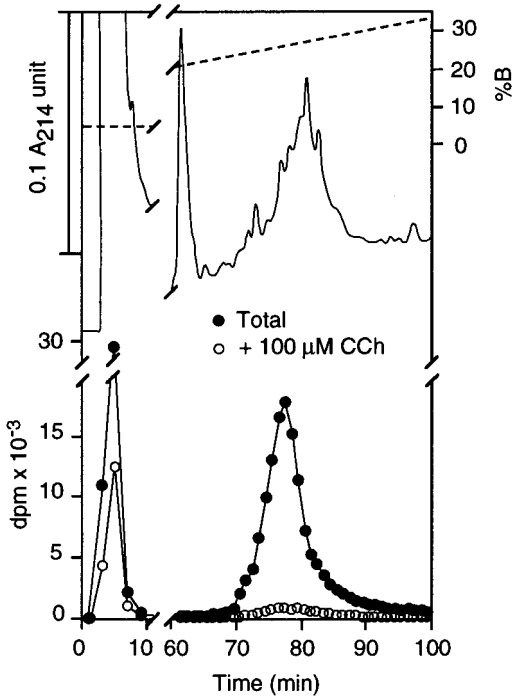

FIGURE 5: Reversed-phase HPLC of CNBr fragments of the [^{3}H]-DCTA-labeled α-subunit subcleaved with trypsin. Large amounts of alkaline-treated membranes (15 nmol, 0.5 μM of α-BgTx binding sites) were irradiated with 10 μM [^{3}H]DCTA in the same conditions as described in Figure 2 in the presence (○) or absence (●) of 100 μM CCh. After "in gel" proteolysis with CNBr (see Materials and Methods), peptides were purified on a Vydac C4 reversed-phase column (4.6 × 250 mm) using the same elution system as described in Figure 2 except that the flow rate was 1 mL/min. The purified peptides were pooled (not shown), neutralized with 2 N NaOH, evaporated under N_2, diluted in 150 mM NH_4HCO_3 pH 7.8 and 30% ACN, and incubated with trypsin (1/50 w/w) for 14 h at 28 °C. The reaction was stopped by acidification with solvent A (0.1% TFA in H_2O), and the mixture was loaded onto a Vydac C4 reversed-phase column (2.1 × 150 mm) equilibrated at 0.2 mL/min with 95% solvent A (0.1% TFA in H_2O) and 5% solvent B (70% 1-propanol, 30% ACN, 0.095% TFA). The elution was performed as mentioned in Figure 2. UV absorbance was monitored at 214 nm, and aliquots of fractions collected were counted for radioactivity. The recovery of injected radioactivity was 75% for the sample irradiated in the absence of CCh. Material contained in fractions 76−79 min was evaporated under N_2 and subjected to sequence analysis.

The sequence αHis-186 corresponded to the expected trypsin cleavage after αLys-185. Although the yield of cleavage with trypsin was quite low (about 10%), it was possible to measure the radioactivity release in the different cycles, showing a strong radioactive increase in cycles 5, 7, and 8 in addition to weaker signals in cycles 12−15 (Figure 6). Thus, the labeled-PTH amino acids observed in cycles 5, 7, and 8 originated from residues αTyr-190, αCys-192, and αCys-193, respectively, within peptide αHis-186. Due to the overlapping sequences, the radioactivity increase observed in cycles 12, 14, and 15 corresponded to the labeling of the same residues αTyr-190, αCys-192, and αCys-193, respectively, in the sequence extending from αLys-179. Furthermore, the radioactive increase observed in cycle 13 does agree with the initially proposed labeling of residue αTyr-198 (within peptide αHis-186). Importantly, this radioactivity increase cannot be attributed to a carryover of the sequencing, since a similar phenomenon should have been observed in cycle 6 within the sequence αHis-186.

Table 2: Yields of PTH Amino Acids upon Sequence Analysis of Trypsin Subcleavage CNBr Peptides[a]

	PTH amino acids (pmol)			
cycle	I	II	III	IV
1	H (NQ)	K (NQ)	E (NQ)	V (NQ)
2	W (ND)	D (4.5)	S (ND)	I (30)
3	V (0.9)	Y (13)	G (3.0)	D (4.8)
4	Y (ND)	R (6.8)	E (2.5)	H (11)
5	Y (0.7)	G (12)	W (0.2)	I (31)
6	T (1.4)	W (0.3)	V (3.0)	L (21)
7	C (ND)	K (2.8)	M (0.2)	L (4.5)
8	C (ND)	H (2.4)	K (NQ)	C (ND)
9	P (0.1)	W (ND)	D (0.4)	V (18)
10	D (3.9)	V (ND)	Y (ND)	F (4.7)
11	T (2.1)	Y (1.0)	R (0.3)	
12	P (0.4)	Y (1.4)	G (1.0)	
13	Y (NQ)	T (1.2)	W (ND)	
14	L(1.0)	C (ND)	K (0.7)	
15	D (3.4)	C (ND)	H (ND)	
16	I (1.7)	P (0.1)	W (ND)	
17	T (0.7)	D (1.0)	V (0.8)	
initial amt (I_0, pmol)	2.8	15	2.6	32
repetitive yield (R, %)	95	83	89	86
starting posn	α186	α179	α172	α405

[a] Same legend as in Table 1.

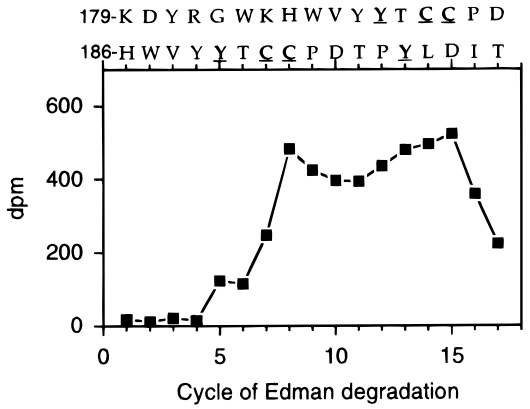

FIGURE 6: Radioactivity released upon sequential Edman degradation of [^{3}H]DCTA-labeled CNBr fragments subcleaved with trypsin. Purified material eluting between 76 and 79 min (Figure 5) was subjected to automated sequence analysis. Radioactivity associated with the PTH fraction at each cycle is shown (■). The loaded sample contained approximately 4×10^4 dpm, of which 12% remained on the filter after 17 cycles. The total radioactivity recovered in the 17 cycles represented 4.8×10^2 dpm (12% of the load). The two identified peptides extending from αLys-179 and αHis-186 are shown, and the radiolabeled amino acids are indicated in underlined and boldface type.

Thus αTyr-190, αCys-192, αCys-193, and also αTyr-198 are most likely the only amino acids specifically labeled by [^{3}H]DCTA in the α-subunit of *Torpedo* nAChR.

DISCUSSION

In the present study we further investigated the photolabeling of the nAChR from *Torpedo* alkaline-treated membranes with the agonist [^{3}H]DCTA (Chart 1), to identify, predominantly in the desensitized state, the specific site of [^{3}H]DCTA photoincorporation at the amino acids level. UV irradiation of nAChR-rich membranes with [^{3}H]DCTA was performed according to the experimental procedure described in Grutter et al. (*16*) and led to photoincorporation into the α- and γ-subunits with satisfactory yields. Irradiation of large amounts of ACh binding sites with [^{3}H]DCTA was undertaken with the prospect of identifying the labeled amino acids.

The concentration-dependence of [^{3}H]DCTA photoincorporation into the α- and γ-subunits was achieved (Figure 1A) up to 50 μM, mainly in the desensitized state (*28*). These incorporations were consistent with a photolabeling reaction occurring on a single population of sites with apparent dissociation constants for labeling K_{app} of 2.2 ± 1.1 and 3.6 ± 2.8 μM, respectively. These values were in good agreement with the reversible dissociation constant value $K_D = 2.6 \pm 0.7$ μM measured previously (*16*). No labeling was observed on the δ-subunit with [^{3}H]DCTA as it was shown with the agonist [^{3}H]nicotine (*8*). The antagonist [^{3}H]-*d*-tubocurarine was demonstrated to bind with a high-affinity at the boundary of the α- and γ-subunits site and with a low-affinity at the boundary of the α- and δ-subunits site (*29*, *30*). Inhibition of [^{3}H]DCTA photolabeling in the α-subunit by *d*-tubocurarine could be interpreted either as a one-site or a two-site interaction model (Figure 1B). Although the two-sites interaction model is preferred (*8*, *30*), our experimental data could not be fitted unambiguously to one of these two models probably because [^{3}H]DCTA photoincorporates into the two ACh binding sites with different efficiency and/or equilibria between [^{3}H]DCTA, nAChR, and *d*-tubocurarine are constantly modified during the photolabeling experiments. When the two-sites model and the stoichiometry of the photoincorporation (one molecule of [^{3}H]DCTA incorporated in an agonist protectable manner per inactivated α-BgTx binding site; see ref *16*) are considered, the data are consistent with the [^{3}H]DCTA molecules bound to the two agonist sites on the α-subunits but showing a preferred accessibility of the photogenerated species for the γ-subunit over the δ-subunit.

Within the α-subunit, CNBr proteolysis followed by HPLC purification of peptides led to a unique carbamylcholine-protected radioactive peak (Figure 2). Microsequencing of the peptides mixture contained in this peak revealed αTyr-190, αCys-192, and αCys-193 as candidate residues for the [^{3}H]DCTA photolabeling reaction (Figure 3). On the basis of microsequence analyses and adjustement for repetitive yield (R = 85%; see Table 1), the radioactivity incorporation would be partitioned equally into αTyr-190, αCys-192, and αCys-193 suggesting that these residues are located with similar proximity to the photoreactive moiety of the [^{3}H]DCTA probe. The identity of the [^{3}H]DCTA-labeled residues was further confirmed by subcleavage of CNBr fragments with trypsin (Figure 5). The expected release of radioactivity in cycles 5, 7, and 8 indicated that residues αTyr-190, αCys-192, and αCys-193 were effectively labeled by [^{3}H]DCTA. The residue αTyr-198 was very likely labeled by [^{3}H]DCTA consistent with the increase of radioactivity observed in cycle 13 (Figure 6). According to the adjustement for repetitive yield (R = 95%, Table 2), the partition of radioactivity which was equal for αTyr-190 and αCys-192 doubled for αCys-193. These differences originated probably from the trypsin subcleavage step, as a strong release of radioactivity was observed in the void volume during HPLC purification (Figure 5), suggesting that some photoadducts may be labile under the trypsinolysis reaction conditions. Because of the difficulty to quantify yields from long sequencing runs, labeling of αTyr-198 could not be standardized precisely to the other labeled residues.

An attempt was made to identify the [^{3}H]DCTA-labeled residue(s) on the γ-subunit. The isolated γ-subunit was proteolyzed "in gel" by trypsin, and peptides were separated by HPLC (data not shown). Unfortunately, due to the extremely low photocoupling yield (1.2%), no release of tritium above background during the tryptic [^{3}H]DCTA-labeled peptide(s) sequencing was detected.

The binding site of ACh on its nicotinic receptor was localized at the boundary of different subunits comprising a main contribution from at least three peptide loops on the α-subunit. The results obtained with the agonist [^{3}H]DCTA, like previous (photo)affinity labels, show that the photoprobe reacted with amino acids contained in loop C of the *Torpedo* α-subunit. The antagonist [^{3}H]DDF (*22*), in the presence of phencyclidine, photoincorporated into αTyr-93 (loop A (*6*)), αTrp-149 (loop B (*5*)), and αTyr-190, αCys-192, αCys-193, and αTyr-198 (loop C (*5*)) defining the ACh binding site as a 12-Å-diameter sphere within the different peptide loops. However, precise structural elements on the interaction of the DDF molecule with the receptor cannot be clearly identified. In the absence of any allosteric effectors, the antagonist [^{3}H]*d*-tubocurarine, which labeled mainly residues from loop C on the α-subunit in addition to γTrp-55,δTrp-57 (*7*) and γTyr-111,γTyr-117 (*12*), reacted with the protein with undefined photochemical reactivity, preventing therefore further structural investigations. A similar example arises from the photolabeling experiments using the agonist [^{3}H]-nicotine identifying precisely loop C residues on the α-subunit (*8*) and to a lesser extent γTrp-55 (*13*). Finally, a chemical coupling was described between coral [^{3}H]lophotoxin analog-1 and αTyr-190 (*9*); however, the identification of the reactive moiety of the toxin remained speculative (*31*).

The affinity label [^{3}H]MBTA alkylated only the ACh binding site under reducing conditions providing first evidence of direct interaction of the ester moiety of ACh with αCys-192 and αCys-193 although in non-native conditions (e.g. after cleavage of the 192−193 disulfide bridge) (*10*). Moreover, the agonist [^{3}H]ACh mustard identified the amino acid αTyr-93 by affinity labeling (*11*). Even though the coupling reaction was weak, this labeling result suggested a direct interaction of the ACh ammonium moiety with residue αTyr-93.

The DCTA molecule offers a strong advantage over most of the used reactive probes on the nicotinic receptor. It first possesses a structure where the analogies with the ACh molecule can be clearly identified; the presence of the quaternary ammonium group provides an anchoring site on the protein and causes the diazocyclohexadienoyl moiety to overlap with the ester part of ACh (Chart 1). Second, the photochemical properties of DCTA are well-defined and are precisely associated to the diazo function generating reactive carbene species, able to insert in carbon−hydrogen bonds (*32*). Since the short-lived carbene intermediates (either singlet or triplet) react with any surrounding amino acid residue, it is postulated that the labeled α-subunit residues are located in the vicinity of the diazocyclohexadienoyl moiety. Furthermore the half-lives of such carbenes have been determined, reaching the subnanosecond level (*33*), so that the high reactivity of these species renders unlikely the labeling of these amino acids after diffusion of the reactive intermediate away from the [^{3}H]DCTA binding site.

All these data suggest that the residues labeled by [^{3}H]-DCTA, αTyr-190, αCys-192, αCys-193, and αTyr-198 contribute to the ACh binding site, matching exactly the residues of the α-subunit labeled by the agonist [^{3}H]nicotine (*8*), and even more precisely, these residues participate directly to the binding of the ester moiety of ACh. The flexibility of the [^{3}H]DCTA molecule associated with the high reactivity of the photogenerated carbene lead to a topographical mapping of most, if not, all amino acids in contact to the photosensitive moiety of [^{3}H]DCTA. By contrast, [^{3}H]nicotine is a semirigid agonist which presents a single possible torsional rotation around the exocyclic σ bond. Assuming that the quaternary ammonium group of [^{3}H]-DCTA and the tertiary amine of [^{3}H]nicotine superimpose within the ammonium subsite, and the fact that these two probes labeled exactly the same residues on the α-subunit, implies a similar contribution of these amino acids in the binding of the ester function of ACh as depicted in Figure 7. The residue(s) weakly labeled with [^{3}H]DCTA on the γ-subunit might also be part of this ester subsite. The remarkable identity between the labeling results of the two agonists [^{3}H]nicotine and [^{3}H]DCTA suggests that the photochemical reaction on nicotine occurred mainly on its pyridine ring. Besides the fact that [^{3}H]DCTA represents an efficient photoaffinity probe, the only difference which could be observed during the labeling reactions is that [^{3}H]nicotine labeled preferentially αTyr-198 (*8*) whereas [^{3}H]DCTA labeled with equal efficiency αTyr-190, αCys-192, and αCys-193. These local divergences may reflect subtle differences in the mode of interactions of these two probes with residues belonging to loop C of the ACh binding site.

The fact that no other amino acids were identifed in the labeling reaction using [^{3}H]DCTA, in particular, αTyr-93 and αTrp-149, suggests that these two residues are not accessible to the photoreactive part of DCTA and do not contribute directly to the binding of the ester fragment but rather to the binding of the ammonium part of the ACh molecule. Indeed, it was shown using the unnatural amino acid incorporation method that αTrp-149 exerted a predominant cation/π interaction with the quaternary ammonium group over the αTyr-93, αTyr-190, and αTyr-198 residues (*34*, *35*). Also, the affinity labeling reaction using the acetylcholine mustard depicted a weak labeling of the αTyr-93 residue, suggesting a proximity of this residue to the ammonium part of ACh (*11*). A positioning of the αTyr-93 and αTrp-149 residues in the ammonium domain on the opposite side of the ester of ACh or the diazocyclohexadienoyl ring of DCTA would accommodate all the labeling results (Figure 7B). Alternatively, site-directed mutagenesis studies done on muscle-type receptors (*36*−*40*) and neuronal receptors (*41*, *42*) pointed out the major role played by the three loops (A−C) and, in particular, aromatic residues in the ACh binding pocket. Mutations done on mouse nAChR expressing 293 HEK cells (*39*) found that the conserved tyrosine residues (αTyr-93, αTyr-190, and αTyr-198) stabilized the quaternary ammonium groups of agonists while αTyr-190 and αTyr-198 were also involved in the binding of curariform antagonists. Despite an apparent discrepancy, these site-directed mutagenesis experiments can be interpreted in the light of our labeling results. While the αTyr-93 residue seems to contribute exclusively to the binding of the ammonium group as proposed earlier, the

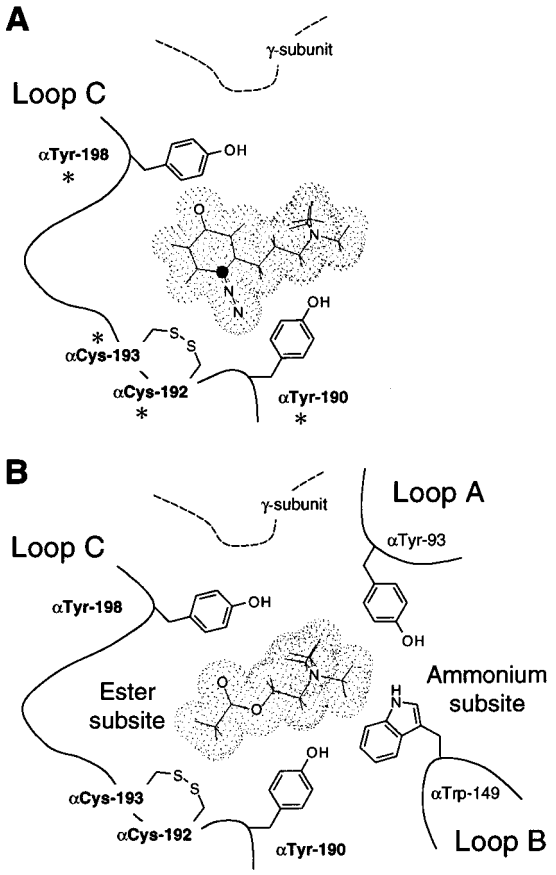

FIGURE 7: Proposed positioning of the DCTA and ACh molecules within the agonist binding site in the desensitized state: identification of the ammonium and ester subsites. (A) Proposed interaction model for [^{3}H]DCTA with labeled residues in loop C of the ACh binding site at the $\alpha-\gamma$ interface. Amino acids labeled with [^{3}H]DCTA were denoted by asterisks. Loop C-labeled residues, αTyr-190, αCys-192, αCys-193, and αTyr-198, are tentatively located in proximity to the photosensitive moiety (●) of [^{3}H]DCTA. (B) Proposed interaction model for the ACh molecule within its site. Loop C-labeled residues are positioned to interact with the ACh ester part which can be overlapped to the diazocyclohexadienoyl ring of DCTA. This subsite is called the ester subsite. Loops A and B containing αTyr-93 and αTrp-149, respectively, not labeled with [^{3}H]DCTA, are proposed to be located in proximity to the quaternary ammonium group of ACh. This subsite is called the ammonium subsite, which, in addition to the αTyr-93 and αTrp-149 residues, could also contain the two tyrosines residues, αTyr-190 and αTyr-198, shared by the two subsites. The γ-subunit, located arbitrarily between the ester and ammonium subsite, is represented in dashed line, and the other site ($\alpha-\delta$ interface) is not represented. DCTA and ACh molecules are depicted in dotted structures.

αTyr-190 and αTyr-198 side chains could, in addition to the binding of the ester part of ACh or diazocyclohexadienoyl ring of DCTA, furthermore interact with the ammonium group as illustrated in the Figure 7B. Indeed, our photolabeling results do not rule out the possibility that some of the identified residues could also participate to the binding of the quaternary ammonium moiety. Interestingly, only the two aromatic residues (αTyr-190 and αTyr-198) in contact with the ester group of ACh seem accessible to the curariform antagonists (*39*).

In summary, we have identified αTyr-190, αCys-192, αCys-193, and αTyr-198 as the amino acids specifically labeled by the agonist [^{3}H]DCTA (Figure 7A). In the absence of a X-ray structure, our labeling results, performed on the native desensitized nAChR, allowed us for the first time to identify the ester and ammonium subsites of ACh and to pinpoint the corresponding amino acids which contribute to these sites. The proposed interaction model (Figure 7B) accounts also for the different results obtained from other groups (*10*, *11*, *35*, *41*) and allows potential refinements of a model which has been built on the bases of the overall site-directed labeling and mutagenesis results (*43*). Finally, the agonistic properties of the DCTA probe open the possibility to investigate, at the molecular level, the allosteric transitions leading to the functional and desensitized states of the nAChR by using rapid mixing techniques coupled to a powerful UV source (*44*). These dynamic photolabeling experiments are presently in progress.

ACKNOWLEDGMENT

We thank M. Leret for technical assistance during sequencing and Dr. B. Foucaud for fruitful discussions.

REFERENCES

1. Changeux, J. P., and Edelstein, S. J. (1998) *Neuron 21*, 959−980.
2. Lukas, R. J., Changeux, J. P., Le Novere, N., Albuquerque, E. X., Balfour, D. J., Berg, D. K., Bertrand, D., Chiappinelli, V. A., Clarke, P. B., Collins, A. C., Dani, J. A., Grady, S. R., Kellar, K. J., Lindstrom, J. M., Marks, M. J., Quik, M., Taylor, P. W., and Wonnacott, S. (1999) *Pharmacol. Rev. 51*, 397−401.
3. Hucho, F., Tsetlin, V. I., and Machold, J. (1996) *Eur. J. Biochem. 239*, 539−557.
4. Corringer, P. J., Bertrand, S., Galzi, J. L., Devillers-Thiery, A., Changeux, J. P., and Bertrand, D. (1999) *Neuron 22*, 831−843.
5. Dennis, M., Giraudat, J., Kotzyba-Hibert, F., Goeldner, M., Hirth, C., Chang, J. Y., Lazure, C., Chretien, M., and Changeux, J. P. (1988) *Biochemistry 27*, 2346−2357.
6. Galzi, J. L., Revah, F., Black, D., Goeldner, M., Hirth, C., and Changeux, J. P. (1990) *J. Biol. Chem. 265*, 10430−10437.
7. Chiara, D. C., and Cohen, J. B. (1997) *J. Biol. Chem. 272*, 32940−32950.
8. Middleton, R. E., and Cohen, J. B. (1991) *Biochemistry 30*, 6987−6997.
9. Abramson, S. N., Li, Y., Culver, P., and Taylor, P. (1989) *J. Biol. Chem. 264*, 12666−12672.
10. Kao, P. N., Dwork, A. J., Kaldany, R. R., Silver, M. L., Wideman, J., Stein, S., and Karlin, A. (1984) *J. Biol. Chem. 259*, 11662−11665.
11. Cohen, J. B., Sharp, S. D., and Liu, W. S. (1991) *J. Biol. Chem. 266*, 23354−23364.
12. Chiara, D. C., Xie, Y., and Cohen, J. B. (1999) *Biochemistry 38*, 6689−6698.
13. Chiara, D. C., Middleton, R. E., and Cohen, J. B. (1998) *FEBS Lett. 423*, 223−226.
14. Kotzyba-Hibert, F., Kessler, P., Zerbib, V., Bogen, C., Snetkov, V., Takeda, K., Goeldner, M., and Hirth, C. (1996) *J. Neurochem. 67*, 2557−2565.
15. Kotzyba-Hibert, F., Kessler, P., Zerbib, V., Grutter, T., Bogen, C., Takeda, K., Hammadi, A., Knerr, L., and Goeldner, M. (1997) *Bioconjugate Chem. 8*, 472−480.
16. Grutter, T., Goeldner, M., and Kotzyba-Hibert, F. (1999) *Biochemistry 38*, 7476−7484.
17. Nachon, F., Ehret-Sabatier, L., Loew, D., Colas, C., van Dorsselaer, A., and Goeldner, M. (1998) *Biochemistry 37*, 10507−10513.
18. Saitoh, T., and Changeux, J. P. (1980) *Eur. J. Biochem. 105*, 51−62.
19. Neubig, R. R., Krodel, E. K., Boyd, N. D., and Cohen, J. B. (1979) *Proc. Natl. Acad. Sci. U.S.A. 76*, 690−694.

20. Schmidt, J., and Raftery, M. A. (1973) *Anal. Biochem. 52*, 349−354.
21. Peterson, G. L. (1977) *Anal. Biochem. 83*, 346−356.
22. Langenbuch-Cachat, J., Bon, C., Mulle, C., Goeldner, M., Hirth, C., and Changeux, J. P. (1988) *Biochemistry 27*, 2337−2345.
23. Rosenfeld, J., Capdevielle, J., Guillemot, J. C., and Ferrara, P. (1992) *Anal. Biochem. 203*, 173−179.
24. Ogorzalek-Loo, R. R., Stevenson, T. I., Mitchell, C., Loo, J. A., and Andrews, P. C. (1996) *Anal. Chem. 68*, 1910−1917.
25. Cordoba, O. L., Linskens, S. B., Dacci, E., and Santome, J. A. (1997) *J. Biochem. Biophys. Methods 35*, 1−10.
26. Schagger, H., Aquila, H., and Von Jagow, G. (1988) *Anal. Biochem. 173*, 201−205.
27. Krodel, E. K., Beckman, R. A., and Cohen, J. B. (1979) *Mol. Pharmacol. 15*, 294−312.
28. Heidmann, T., Oswald, R. E., and Changeux, J. P. (1983) *Biochemistry 22*, 3112−3127.
29. Blount, P., and Merlie, J. P. (1989) *Neuron 3*, 349−357.
30. Pedersen, S. E., and Cohen, J. B. (1990) *Proc. Natl. Acad. Sci. U.S.A 87*, 2785−2789.
31. Abramson, S. N., Trischman, J. A., Tapiolas, D. M., Harold, E. E., Fenical, W., and Taylor, P. (1991) *J. Med. Chem. 34*, 1798−1804.
32. Alcaraz, M. L., Peng, L., Klotz, P., and Goeldner, M. (1996) *J. Org. Chem. 61*, 192−201.
33. Arnold, B. R., Scaiano, J. C., Bucher, G. F., and Sander, W. W. (1992) *J. Org. Chem. 57*, 6469−6474.
34. Kearney, P. C., Nowak, M. W., Zhong, W., Silverman, S. K., Lester, H. A., and Dougherty, D. A. (1996) *Mol. Pharmacol. 50*, 1401−1412.
35. Zhong, W., Gallivan, J. P., Zhang, Y., Li, L., Lester, H. A., and Dougherty, D. A. (1998) *Proc. Natl. Acad. Sci. U.S.A. 95*, 12088−12093.
36. O'Leary, M. E., and White, M. M. (1992) *J. Biol. Chem. 267*, 8360−8365.
37. Aylwin, M. L., and White, M. M. (1994) *FEBS Lett. 349*, 99−103.
38. Aylwin, M. L., and White, M. M. (1994) *Mol. Pharmacol. 46*, 1149−1155.
39. Sine, S. M., Quiram, P., Papanikolaou, F., Kreienkamp, H. J., and Taylor, P. (1994) *J. Biol. Chem. 269*, 8808−8816.
40. McLaughlin, J. T., Hawrot, E., and Yellen, G. (1995) *Biochem. J. 310*, 765−769.
41. Galzi, J. L., Bertrand, D., Devillers-Thiery, A., Revah, F., Bertrand, S., and Changeux, J. P. (1991) *FEBS Lett. 294*, 198−202.
42. Corringer, P. J., Bertrand, S., Bohler, S., Edelstein, S. J., Changeux, J. P., and Bertrand, D. (1998) *J. Neurosci. 18*, 648−657.
43. Tsigelny, I., Sugiyama, N., Sine, S. M., and Taylor, P. (1997) *Biophys. J. 73*, 52−66.
44. Kotzyba-Hibert, F., Grutter, T., and Goeldner, M. (1999) *Mol. Neurobiol. 20*, 45−59.

BI992393O